Control Systems Analysis of a Multiscale Simulation Code for Copper Electrodeposition

Effendi Rusli, Timothy O. Drews, and Richard D. Braatz, *Member*, *IEEE*

Abstract—**Multiscale systems involve phenomena that span several orders of magnitude in time and length scales, from the molecular to the macroscopic. To account for the multiscale character of these processes, many papers have adopted a simulation architecture that employs coupled simulation codes, in which each code simulates the physicochemical phenomena for a different range of length scales. A key issue in dynamically coupling simulation codes is that it is possible for the codes that solve the individual continuum or non-continuum models to be numerically stable, while the dynamic linkage of the individual codes is numerically unstable. This paper uses control systems analysis to gain insight into these numerical instabilities as well as to design numerical linkage algorithms that modify the dynamic information passed between the individual codes to numerically stabilize their coupling, and to increase the numerical accuracy of the simulation results. The approach is applied to a coupled KMC-FD code for simulating copper electrodeposition in sub-micron trenches.**

I. Introduction

New applications in materials, medicine, and computers are being discovered where the control of events at the molecular and nanoscopic length scales is critical to product quality, although the primary manipulation of these events during processing occurs at macroscopic length scales (e.g., the temperature of the system, the valve positions on flows into and out of the system, an applied potential between two electrodes). These applications include nanobiological devices, micromachines, nanoelectronic devices, and protein microarrays and chips [3],[8],[9],[12]-[14].

Many chemical reaction modeling papers have adopted a multiscale simulation architecture that employs coupled simulation codes, in which each code simulates the physicochemical phenomena for a different range of length scales. Vlachos [17] linked a surface Monte Carlo model and a fluid-phase continuum reaction/transport model, resulting in a multiscale integration hybrid algorithm to simulate homogeneous/heterogeneous processes. Hansen *et al.* [7] incorporated molecular dynamics data into a level set model to simulate the multiscale growth of an aluminum film. A coupled molecular dynamics and Monte Carlo simulation code was used to improve feature-scale simulations of the ionized physical vapor deposition of copper in a trench; the ion sticking probabilities which are location dependent were supplied by a molecular dynamics code to a Monte Carlo code that simulated the trench in-fill [2]. Linked codes have been used to simulate Metal-Oxide Semiconductor Field Effect Transistors (MOSFETs) in which a Monte Carlo code computes the electron transport across the MOS which is sent to a finite element (continuum) code that computes the potential and electric field distribution [6]. The output of the finite element code was sent back to the Monte Carlo code, and the calculations were repeated iteratively until convergence was obtained. Gobbert *et al.* [5] simulated low pressure chemical vapor deposition by linking a reactor scale code, a feature scale code, and a mesoscale code that mediated the linkage between the other codes. Pricer *et al.* [10] externally linked a coarse-grained kinetic Monte Carlo (KMC) code and a finite difference (FD) code to simulate copper electrodeposition in a variety of surface geometries and studied the additive effects on morphology evolution. Drews *et al.* [4] developed a code-coupling algorithm that mediated the boundary conditions dynamically passed between the KMC and FD codes, to suppress numerical instabilities and improve the accuracy of the linked simulation.

A key issue in coupling multiscale codes is that it is possible for the codes that solve the individual continuum or non-continuum models to be numerically stable, while the dynamic coupling of the individual codes is numerically unstable. As an illustrative example, consider the multiscale simulation of the copper electrodeposition process, which is used in the manufacture of on-chip interconnects for semiconductor devices [1]. The process involves phenomena that span several orders of magnitude in time and length scales. An accurate description of the deposition process should simultaneously capture the

Manuscript submitted March 12, 2004 for review. This work was supported by the National Science Foundation under grant numbers CTS-0135621, CISE-9619019, and PACI NRAC MCA-01S022

E. Rusli is with the University of Illinois at Urbana-Champaign, IL 61801, USA (e-mail: rusli@uiuc.edu).

T.O. Drews is with the University of Illinois at Urbana-Champaign, IL 61801, USA (e-mail: todrews@uiuc.edu).

R.D. Braatz is with the University of Illinois at Urbana-Champaign, IL 61801, USA (phone: 217-333-5073; e-mail: braatz@uiuc.edu).

macroscopic transport phenomena of all species in the bulk and the surface phenomena at the working electrode, to resolve key structural properties of copper deposits on the length scales from nanometers to tenths of microns. The final product quality is determined by deposit shape and morphology. The time scales characterizing the deposition process range from a few milliseconds in the electrolytic solution to nanoseconds at the electrode surface.

Figure 1 shows the information flow between the finite difference (FD) and kinetic Monte Carlo (KMC) simulation codes dynamically coupled by Drews *et al.* [4]. At each coupling time instance, the KMC code passes to the FD code the vector of species concentrations, c, at the interface between the FD and KMC spatial domains, and the FD code passes the vector of interface fluxes, f, to the KMC code. The dynamically coupled codes with a coupling time step of 5 ms showed the presence of a numerical instability (see Figure 2). Choosing a much smaller time step to avoid the numerical instability would make the coupled simulation very computationally expensive without providing enhanced resolution of time scales in the FD code [4].

The main purpose of this paper is to show how control systems theory can be used to analyze and design numerically stable multiscale code-coupling algorithms. First, it is shown how to write a multiscale simulation code in the operator form used in systems theory (shown in Figure 3). Then nonlinear systems theory is used to make precise statements regarding the well-posedness and numerical stability of dynamically coupled simulation codes. These statements include a constructive procedure for verifying that the dynamic coupling of simulation codes is well-posed, a sufficient condition for the numerical stability of dynamically coupled simulation codes, and a discussion on what can be learned about the input-output behavior of the individual simulation codes from the results of the dynamically coupled simulation. Then systems theory is used to provide guidance for the design of numerically stable algorithms for dynamically coupling simulation codes. The results are illustrated by application to the multiscale simulation of the electrodeposition of copper into a trench.

II. Writing Multiscale Simulation Codes in Operator Form

Any interconnection of dynamically coupled simulation codes can be written in operator or "block diagram" form. Each block represents an operator between the input and output of each simulation code, and the lines between the blocks represent the transfer of information between simulation codes. This approach is applicable regardless of the time scales, length scales, or numerical algorithm used in each simulation code, including whether each simulation algorithm is deterministic or stochastic. To illustrate these points, consider the dynamic coupling used in the multiscale simulation of the copper electrodeposition problem in Figure 1. The input-output behavior of the FD code can be written as $f = H_{FD}\, c$ where the operator H_{FD} is the mapping between the inputs and outputs of the FD code. To write the KMC code in operator form, note that it has an additional input which is implicit in any Monte Carlo code (not shown in Figure 1), which is the random signal ϑ used to select between possible events in the KMC code. In this particular application, the KMC domain includes events that occur at much smaller time scales than the FD domain, so the KMC code iterates for many thousands of iterations before sending its outputs to the FD code. The input-output behavior of the KMC code can be written as $y_2 = H_{KMC}\, e_2$, where $e_2 = [f^{\mathrm{T}}\ \eta^{\mathrm{T}}\ \vartheta^{\mathrm{T}}]^{\mathrm{T}}$ and $y_2 = [c^{\mathrm{T}}\ j^{\mathrm{T}}]^{\mathrm{T}}$. The dynamically coupled code is written in the block diagram form in Figure 3 by defining $H_1 = \mathrm{diag}\{H_{FD}, 0\}$, $H_2 = H_{KMC}$, $y_1 = [f^{\mathrm{T}}\ 0^{\mathrm{T}}]^{\mathrm{T}}$, $e_1 = y_2$, $u_1 = 0$, $u_2 = [0^{\mathrm{T}}\ \eta^{\mathrm{T}}\ \vartheta^{\mathrm{T}}]^{\mathrm{T}}$, and $e_2 = u_2 + y_1$, where 0 is the vector of zeros defined so that the dimensions are consistent. Note that this dynamic coupling in Figure 1 is multi-rate, in that many events occur in the KMC code before the interface concentrations are passed to the FD code. This results in no change in the operator representation in the system, provided that the stochastic signal, ϑ, which changes at the much shorter time interval of the KMC code, is stacked into a vector and the operator H_{KMC} refers to the mapping from the inputs to outputs of the KMC code at each coupling time instance. Then the operator form represents the dynamics at the coupling time instances rather than the KMC time instances. This is the standard lifting approach for addressing multi-rate systems using single-rate analysis [11].

III. Well-posedness of Dynamically Coupled Simulation Codes

As the simulation proceeds, each signal (i.e., e, y, and u in Figure 3) is a sequence of the form $x = \{x_t,\ t = 0, 1, \ldots\}$, where the index t corresponds to the time instant in which the simulation codes pass information, with x_t belonging to the real vector space of dimension n, denoted by R^n. The first question that arises in analysis of dynamically coupled simulation codes is whether their interconnection is well-posed, that is, whether all signals exist and are unique for any choice of inputs to the coupled codes. For example, the coupling in Figure 3 is well-posed if the solutions for the sequences $\{e_t\}$ and $\{y_t\}$ exist and are unique for any choice of sequence $\{u_t\}$. A simulation code is *causal* if the value of the output of time t depends only on the values of the inputs up to time t. Any reasonable implementation of a simulation code for a physical system will be causal. A simulation code is *strictly causal* if the output at time t is a

function only of the simulation inputs for the times strictly less than t. Strict causality is equivalent to having the simulation output require some time to respond to changes in its input. Any simulation code that uses an explicit solver for time-stepping is strictly causal. Theorem 2 of Ref. [16] gives a constructive procedure for testing the well-posedness of an arbitrary interconnection of discrete-time nonlinear operators. When applied to an arbitrary interconnection of simulation codes, the sufficient conditions for well-posedness are that: (i) all simulation codes are causal, (ii) some are strictly causal, and (iii) a reduced digraph constructed from this information as well as the pathways of information flow between codes does not contain any cycles or self-loops (see Ref. [16] for details). Lemma 1 specializes the conditions to the interconnection in Figure 3.

Lemma 1. *The coupled system in Figure 3 is well-posed if both simulation codes* H_1 and H_2 *are causal and one of the simulation codes is strictly causal.*

IV. Numerical Stability of Dynamically Coupled Simulation Codes

The next question arising in the analysis of dynamically coupled simulation codes is whether the interconnection of simulation codes is numerically stable.

Definition 1. *Let* $x \in l_p$. *The operator* H *is* l_p-stable with finite gain $\gamma(H)$ *if there exist nonnegative constants* $\gamma(H)$ and $\beta(H)$ *such that*

$$\|Hx\|_{l_p} \le \gamma(H)\|x\|_{l_p} + \beta(H).$$

For brevity, the term "l_p-stable" is used in this paper to refer to "l_p-stable with finite gain". The integer p in the above definitions is selected as a matter of convenience. Checking whether a simulation code is l_∞-stable is especially easy to test, since all this means is that the simulation outputs are bounded for bounded simulation inputs. Another relatively easy check is whether a simulation code is l_2-stable, as this just means that the simulation outputs have bounded energy for all simulation inputs with bounded energy. For example, the input-output operator for a code that simulates a chemical reactor with an endothermic chemical reaction with no electrochemical reactions is l_2-stable, for any configuration (e.g., stirred, packed bed) and any choice of simulation inputs and outputs (e.g., concentrations, fluxes). To understand this, an endothermic reaction does not liberate heat, and convection and diffusion only move energy around in the reactor. The only energy introduced into the reactor would be the work due to stirring, which is much smaller than the energy taken up by the endothermic reaction. An example of a simulation code that would not be l_p-stable, for any p, is a code for a highly exothermic chemical reactor whose input is the feed flow rate and whose output is the reactor temperature, designed with a heat transfer system that allows ignition (also referred to as reaction runaway) to occur. In such a simulation code, a bounded variation in the simulation input can lead to an unbounded variation in a simulation output.

For brevity, the focus here is on the coupling of two simulation codes that pass updated boundary conditions at a shared interface between the physical domains simulated by the two codes. Similar results hold when more than two simulation codes are dynamically coupled, including when there is spatial overlap between domains. A sufficient condition for numerical stability of two dynamically coupled codes is given by the small gain theorem.

Theorem 1 (Small Gain Theorem). *Consider the interconnected system in Figure 3. Suppose that the operators* H_1 *and* H_2 *are causal and* l_p*-stable*:

$$\|H_1 x_1\|_{l_p} \le \gamma(H_1)\|x_1\|_{l_p} + \beta(H_1),$$

$$\|H_2 x_2\|_{l_p} \le \gamma(H_2)\|x_2\|_{l_p} + \beta(H_2),$$

where $\gamma(H_1)$, $\gamma(H_2)$, $\beta(H_1)$, $\beta(H_2) \ge 0$ *and* $p \in [1,\infty]$. *Then the system in Figure 3 is* l_p*-stable if* $\gamma(H_1)\gamma(H_2) < 1$.

As an example application, for the coupled KMC-FD codes described in Figure 1, both simulation codes are causal since the codes were constructed from first-principles models, and l_∞-stable since the codes produce bounded outputs for bounded inputs (each individual code is numerically stable and the physical systems do not have variables that "blow up"). Then Theorem 1 gives that a sufficient condition for numerical stability is that $\gamma(H_{FD})\gamma(H_{KMC}) < 1$, which is the product of the gains for the individual simulation codes.

The direct application of Theorem 1 to analyze the numerical stability of dynamically coupled simulation codes is limited by the difficulty in computing the gains, $\gamma(H_i)$, for a complex simulation code. However, the contrapositive to Theorem 1 provides information on the input-output behavior of two simulation codes when their dynamic coupling leads to a numerical instability.

Corollary 1. *Consider the interconnected system in Figure 3. Suppose that the operators* H_1 *and* H_2 *are causal and* l_p*-stable*:

$$\|H_1 x_1\|_{l_p} \le \gamma(H_1)\|x_1\|_{l_p} + \beta(H_1),$$

$$\|H_2 x_2\|_{l_p} \le \gamma(H_2)\|x_2\|_{l_p} + \beta(H_2),$$

where $\gamma(H_1)$, $\gamma(H_2)$, $\beta(H_1)$, $\beta(H_2) \ge 0$ *and* $p \in [1,\infty]$. *Then* $\gamma(H_1)\gamma(H_2) > 1$ *if the interconnected system in Figure 3 is not* l_p*-stable*.

Application of Corollary 1 to the KMC-FD codes indicates that $\gamma(H_{FD})\,\gamma(H_{KMC}) > 1$, that is, the product of the gains of the FD and KMC codes are positive. As the practical application of this result, it is well-known that introducing a filter can reduce the gain of a system, that is, a filter F can be designed such that $\gamma(FH_i) < \gamma(H_i)$. This suggests that inserting a filter into Figure 1, to give Figure 4, may numerically stabilize a dynamically coupled simulation code. This is precisely the approach taken by Drews *et al.* [4] to numerically stabilize the coupled FD-KMC simulation codes in Figure 1. The next section applies control systems theory to guide the design of this filter, F, to numerically stabilize the dynamically coupling of two simulation codes, while minimizing its effect on the true dynamics of the multiscale system.

V. Design of a Numerically Stable Code-Coupling Algorithm

Although the overall approach taken here applies to general interconnections of coupled simulation codes, for brevity and illustration purposes, this paper will focus on the application to the coupled codes in Figures 1 and 3. In this section H_1 and H_2 in Figure 3 refer to the operators describing the real physical systems, with $H_{1c}=(I+W_1\Delta_1)H_1$ and $H_{2c}=(I+W_2\Delta_2)H_2$ referring to the operators describing the corresponding simulation codes which provide numerical approximations of the input-output behavior of the real physical systems. As is standard in robust control theory [15], Δ_i are unitary norm-bounded perturbation operators with weights W_i selected to be minimum phase and stable linear time invariant operators that quantify the approximation error between the real physical systems and the corresponding simulation codes. The weights W_i have a low response at low frequencies (which means that the simulation codes accurately capture long time behavior) and high response at high frequencies (or short time behavior, where the simulation codes are expected to be less accurate).

The following assumptions are made: (i) the operators H_1, H_2, F, W_1, W_2, Δ_1, and Δ_2 are l_p-stable, (ii) the interconnection in Figure 3 is well-posed and l_p-stable. Assumption (ii) implies that the variables in the real physical system are well-posed and do not "blow up" for bounded inputs. As is typical when studying robust control problems, linear systems theory will be used to design a compensator (in this case, the filter F) based on linearizations of the nonlinear operators, so henceforth H_1 and H_2 refer to the linearized operators.

With the definitions $y = [y_1^{\mathrm{T}}\ y_2^{\mathrm{T}}]^{\mathrm{T}}$ and $u = [u_1^{\mathrm{T}}\ u_2^{\mathrm{T}}]^{\mathrm{T}}$ in Figure 3, the mapping from u to y, $y = N_T u$, is given by

$$N_T = \begin{bmatrix} (I - H_1H_2)^{-1}H_1 & (I - H_1H_2)^{-1}H_1H_2 \\ H_2(I - H_1H_2)^{-1}H_1 & H_2(I - H_1H_2)^{-1} \end{bmatrix} \quad (1)$$

where I is the identity operator of appropriate dimensions. Assumption (ii) implies that the operator N_T is l_p-stable. It is assumed that the coupled simulation codes are numerically unstable, so that the interconnection in Figure 3 is not l_p-stable when H_1 and H_2 are replaced by H_{1c} and H_{2c}. The goal of the filter F in Figure 5 is to numerically stabilize the coupled codes, which means to stabilize the interconnection in Figure 5 for all allowed perturbations $\Delta_i \in \Delta$, while maintaining consistency between the real physical system and the coupled simulation codes. In general a filter could be located at the output of each simulation code; here the filter was located only at the output of the KMC code, because the KMC code is not as accurate as the FD code in describing the behavior of the real physical system, and that such a filter location has the additional advantage of directly suppressing the effects of KMC simulation noise on the dynamics of the coupled codes.

Theorem 2. *Consider the block diagram in Figure 5 under Assumptions (i) and (ii). Let $d_1, d_2 \in R^1$ be positive. Suppose that there exists a constant $k > 0$ such that the following conditions hold:*

(a) *the interconnection in Figure 3 is well-posed and l_p-stable,*

(b) *the interconnection in Figure 4 is well-posed and l_p-stable,*

(c) $\max\{\gamma(W_1), \gamma(FW_2)\} < k$

(d) $\inf_{d_1,d_2>0} \gamma\left(DN_1D^{-1}\right) < 1/k$,

where $D = \mathrm{diag}\{d_1 I, d_2 I\}$ and

$$N_1 = \begin{bmatrix} (I - H_1FH_2)^{-1}H_1FH_2 & (I - H_1FH_2)^{-1}H_1 \\ H_2(I - H_1FH_2)^{-1} & H_2(I - H_1FH_2)^{-1}H_1 \end{bmatrix} \quad (2)$$

Then the interconnection in Figure 5 is l_p-stable for all unitary norm-bounded perturbations,

$$\Delta_i \in \mathbf{\Delta} = \{\Delta : \gamma(\Delta) \le 1, \beta(\Delta) = 0\}.$$

Proof. The input-output mapping in Figure 5 can be written as

$$\hat{y} = (I - N_1N_w\Delta)^{-1}N_2u \quad (3)$$

where $N_w = \mathrm{diag}\{W_1, FW_2\}$, $\Delta = \mathrm{diag}\{\Delta_1, \Delta_2\}$, and

$$N_2 = \begin{bmatrix} (I - H_1FH_2)^{-1}H_1 & (I - H_1FH_2)^{-1}H_1FH_2 \\ H_2(I - H_1FH_2)^{-1}H_1 & H_2(I - H_1FH_2)^{-1} \end{bmatrix} \quad (4)$$

Condition (b) implies that N_1 and N_2 are l_p-stable. Hence the interconnection in Figure 5 is l_p-stable if and only if $(I - N_1N_w\Delta)^{-1}$ is l_p-stable

$\leftrightarrow D^{-1}\left(I - DN_1D^{-1}DN_w\Delta D^{-1}\right)^{-1}D$ is l_p-stable

$\leftrightarrow \left(I - DN_1D^{-1}DN_w\Delta D^{-1}\right)^{-1}$ is l_p-stable

$\leftarrow \gamma\left(DN_1D^{-1}\right)\gamma\left(DN_w\Delta D^{-1}\right) < 1$

$\leftrightarrow \gamma\left(DN_1D^{-1}\right)\gamma\left(N_wD\Delta D^{-1}\right) < 1$

$\leftarrow \gamma\left(DN_1D^{-1}\right)\gamma\left(N_w\right)\gamma\left(D\Delta D^{-1}\right) < 1$

$\leftarrow \gamma\left(D\Delta D^{-1}\right) < 1,\ \gamma\left(N_w\right) < k\ ,\ \gamma\left(DN_1D^{-1}\right) < 1/k$

$\leftarrow \gamma(\Delta) < 1,\ \gamma\left(W_1\right) < k,\ \gamma\left(FW_2\right) < k,\ \gamma\left(DN_1D^{-1}\right) < 1/k,$

where the fourth relation follows from Theorem 1. (QED)

Recall that condition (a) in Theorem 2 just states that the interconnection of the real physical systems is well-posed and does not have signals that "blow up" with time. As discussed earlier, condition (a) is a mild condition. Condition (b) states that the interconnection of the real physical systems is well-posed and does not have signals that "blow up" with time when a filter introduced into the system. For the design reasons discussed below, the filter F is selected to be low pass. If the filter is selected to be the linear time invariant system with the transfer function $\hat{F}(s) = 1/(\lambda s + 1)^m$, where m is a positive integer, then a physical process with this transfer function is m equivalent well-mixed processes in series. That is, the introduction of this filter F into the physical system would introduce a lag into the dynamics of the interconnected system, which for a physical system is not likely to introduce instability. That is, condition (b) is very likely to hold if condition (a) holds. The next lemma shows that condition (b) in Theorem 2 is obtained "for free" when l_p-stability of the interconnection in Figure 3 can be proved using the small gain theorem.

Lemma 2. *Suppose that the interconnection in Figure 3 is well-posed and l_p-stable, that the operators H_1 and H_2 are l_p-stable and causal, the filter F is strictly causal, and that $\gamma(F) \le 1$ and $\gamma(H_2H_1) < 1$. Then the interconnection in Figure 4 is well-posed and l_p-stable.*

Proof. The well-posedness is given by Lemma 1. The l_p-stability of the system follows from Theorem 1 and some algebraic manipulation. (QED)

Condition (c) of Theorem 2 quantifies the differences in input-output behavior of the real physical systems and the simulation codes, and motivates the positioning of the filter F at the output of the KMC code. The weights W_i should be selected to be high pass for most simulation codes, since the input-output behavior of a simulation code deviates from that of the real physical system for the shortest time scales. This behavior, which occurs for nearly any model for a real physical system, is typical of *unmodeled dynamics* as described in papers on robust control applications. In the coupled KMC-FD code, the uncertainties associated with the KMC code were rather large, so the filter F is positioned so that it can reduce the effects of these uncertainties on the coupled system. The filter F should be tuned based on condition (c), since F has a more direct effect on the gain in condition (c) than the gain in condition (d). Condition (c) indicates that the filter F should be designed to suppress the effects of the uncertainties of the KMC code, which are quantified by the high pass weight W_2. Since both W_2 and F are linear time invariant, even when the operators H_i are nonlinear, the filter F can be designed by plotting FW_2 in the frequency domain, and selecting the dynamics of F to roll off at the frequencies where the uncertainties in the KMC code are considered likely to be significant (where $|W_2(e^{-j\omega})|$ is large), so that $\gamma(FW_2)$ is significantly less than $\gamma(W_2)$.

Algorithms exist for solving the optimization in condition (d) (e.g, see [15]). Conditions (c) and (d) can be used to show that the simulation codes are numerically stabilized if sufficient filtering is performed. The next result considers tuning F for numerical accuracy.

Theorem 3. *Define M by $\tilde{y} - y = Mu$ and $\gamma_2(M)$ as the gain of M for $p = 2$, where y is the vector of outputs of the real physical system defined in Figure 3 and $\tilde{y}$ is the vector of outputs defined in Figure 5. Then $\gamma_2(M) < k$ if the conditions of Theorem 2 are satisfied with $p = 2$ and*

$$\inf_{d_1, d_2 \neq 0} \gamma_2\left(D\begin{bmatrix} N_1N_w & N_2 \\ k^{-1}(I + N_1)N_w & k^{-1}\left(N_2 - N_T\right) \end{bmatrix}D^{-1}\right) < 1 \tag{5}$$

where $D = \mathrm{diag}\{d_1I, d_2I\}$.

Proof. Block diagram manipulation and robust performance theory [15] gives the condition in (5). (QED)

Since this robust performance problem has quite a different form from what is typically encountered in robust controller synthesis, it is worthwhile to check consistency for the case when the perturbations are negligible ($N_w \approx 0$). In this case (5) simplifies to

$$\gamma_2\left(N_2 - N_T\right) < k. \tag{6}$$

Hence for nominal performance a filter designed to minimize the error $\tilde{y} - y$ should minimize the left hand side of (6). As the operator N_T reduces to N_2 when $F = I$, the code-coupling filter should be designed to be equal to the identity operator except for frequencies where the weight W_2 is large. This agrees with engineering intuition. As another consequence of (5) and (6), a filter designed to barely achieve numerical stability of the coupled codes does not yield simulation results that are most consistent with the real physical system. Although Theorems 2 and 3 were derived from linearized operators, the theorems suggest guidelines for general nonlinear simulation codes, that is, that F should be designed as a low-pass filter that

rolls off at the frequencies where the uncertainties are considered likely to be significant.

VI. Conclusions

This paper showed how control systems theory can be used to design numerical algorithms for coupling dynamic simulation codes. Nonlinear systems theory provided a constructive procedure for testing whether an arbitrary interconnection of simulation codes is well-posed, and a sufficient condition for the numerical stability of dynamically coupled simulation codes.

Linear systems theory provided guidelines for the design of a code-coupling filter for a pair of dynamically coupled FD-KMC codes for simulating a multiscale copper electrodeposition process. Systems theory elucidated the tradeoff in filter design between providing numerical stability and numerical accuracy.

Acknowledgment

Any opinions, findings, and conclusions or recommendations expressed in this paper are those of the authors and do not necessarily reflect the views of the National Science Foundation.

References

[1] P.C. Andricacos, "Copper On-Chip Interconnections – A Breakthrough in Electrodeposition to Make Better Chips," *The Electrochemical Society Interface*, vol. 8, pp. 32, 1999.

[2] D.G. Coronell, D.E. Hansen, A.F. Voter, C. Liu, X. Liu, and J.D. Kress, "Molecular Dynamics-Based Ion-Surface Interaction Modes for Ionized Physical Vapor Deposition Feature Scale Simulations," *Appl. Phys. Lett.*, vol. 73, pp. 3860, 2000.

[3] K.E. Drexler, *Nanosystems: Molecular Machinery, Manufacturing, and Computation*, Wiley Interscience, New York, 1992.

[4] T.O. Drews, E.G. Webb, D.L. Ma, J. Alameda, R.D. Braatz, and R.C. Alkire, "Coupled Mesoscale-Continuum Simulations of Copper Electrodeposition in a Trench," *AIChE J.*, vol. 50, pp. 226, 2004.

[5] M.K. Gobbert, T.P. Merchant, L.J. Borucki, and T.S. Cale, "A Multiscale Simulator for Low Pressure Chemical Vapor Deposition," *J. Electrochem. Soc.*, vol. 144, pp. 3945, 1997.

[6] D. Hadji, Y. Marechal, and J. Zimmerman, "Finite Element and Monte Carlo Simulation of Submicrometer Silicon n-MOSFET's," *IEEE Trans. on Magnetics*, vol. 35, pp. 1809, 1999.

[7] U. Hansen, S. Rodgers, and K.F. Jensen, "Modeling of Metal Thin Film Growth: Linking Angstrom-scale Molecular Dynamics Results to Micron-scale Film Topographies," *Phys. Rev. B*, vol. 62, pp. 2869, 2000.

[8] M. Hoummady, and H. Fujita, "Micromachines for Nanoscale Science and Technology," *Nanotechnology*, vol. 10, pp. 29, 1999.

[9] S.Y. Lee, S.J. Lee, and H.T. Jung, "Protein Microarrays and Chips," *J. Ind. Eng. Chem.*, vol. 9, pp. 9, 2003.

[10] T.J. Pricer, M.J. Kushner, and R.C. Alkire, "Monte Carlo Simulation of the Electrodeposition of Copper - Parts I and II," *J. Electrochem. Soc.*, vol. 149, pp. C396, 2002.

[11] L. Qiu, and K. Tan, "Direct State Space Solution of Multirate Sampled-data H-2 Optimal Control," *Automatica*, vol. 34, pp. 1431, 1998.

[12] A. Prokop, "Bioartificial Organs in the Twenty-first Century-Nanobiological Devices," *Bioartificial Organs III: Tissue Sourcing, Immunoisolation, and Clinical Trials, Annals of the New York Academy of Sciences*, vol. 944, pp. 472, 2001.

[13] "International Technology Roadmap for Semiconductors," International Sematech, 2002.

[14] K. Tsukagoshi, N. Yoneya, S. Uryu, Y. Aoyagi, A. Kanda, Y. Ootuka, and B.W. Alphenaar, "Carbon Nanotube Devices for Nanoelectronics," *Physica B-Condensed Matter*, vol. 323, pp. 107, 2002.

[15] K. Zhou, J.C. Doyle, and K. Glover, *Robust and Optimal Control*, Prentice Hall, Upper Saddle River, New Jersey, 1996.

[16] M. Vidyasagar, "On the Well-posedness of Large-scale Interconnected Systems," *IEEE Trans. Autom. Control*, vol. AC-25, pp. 413, 1980.

[17] D.G. Vlachos, "Multiscale Integration Hybrid Algorithms for Homogeneous-Heterogeneous Reactors," *AIChE J.*, vol. 43, pp. 3031, 1997.

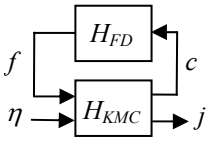

Fig. 1. Dynamic coupled FD-KMC codes used to simulate an electrodeposition process: η is the applied potential, and j is the current density.

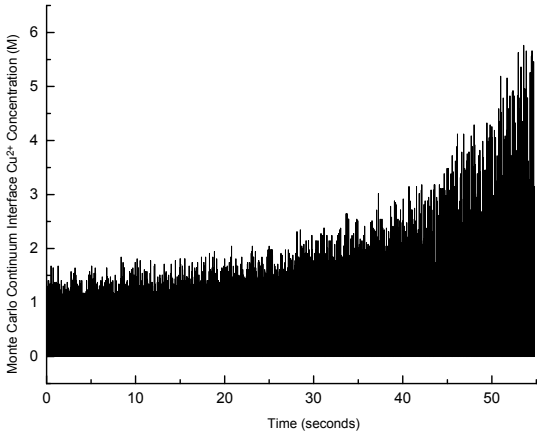

Fig. 2. An interface concentration, c_i, as a function of time, indicating a numerical instability (for details, see Ref. [4]).

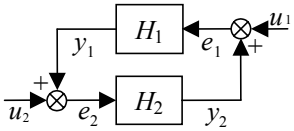

Fig. 3. Coupled operators, with $x_t = [x_{1,t}{}^{\mathrm{T}}\ x_{2,t}{}^{\mathrm{T}}]^{\mathrm{T}}$ for $x = u, e, y$.

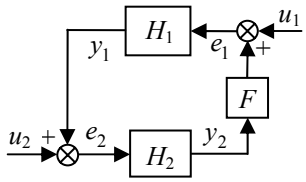

Fig. 4. Interconnected system that incorporates the code-coupling filter F.

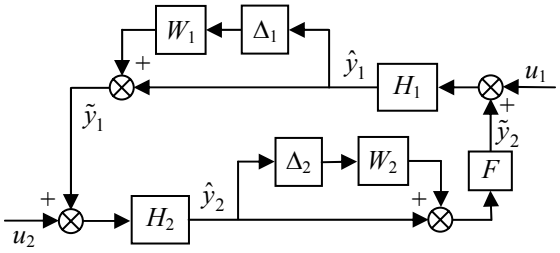

Fig. 5. Interconnected systems with perturbations used in the filter analysis.